Kinetic and Crystallographic Analysis of the Key Active Site Acid/Base Arginine in a Soluble Fumarate Reductase†

Christopher G. Mowat,‡,§ Ruth Moysey,‡ Caroline S. Miles,§ David Leys,‡,§ Mary K. Doherty,‡ Paul Taylor,§ Malcolm D. Walkinshaw,§ Graeme A. Reid,§ and Stephen K. Chapman*,‡

Department of Chemistry, University of Edinburgh, West Mains Road, Edinburgh EH9 3JJ, U.K., and Institute of Cell and Molecular Biology, University of Edinburgh, Mayfield Road, Edinburgh EH9 3JR, U.K.

Received June 28, 2001; Revised Manuscript Received August 6, 2001

ABSTRACT: There is now overwhelming evidence supporting a common mechanism for fumarate reduction in the respiratory fumarate reductases. The X-ray structures of substrate-bound forms of these enzymes indicate that the substrate is well positioned to accept a hydride from FAD and a proton from an arginine side chain. Recent work on the enzyme from *Shewanella frigidimarina* [Doherty, M. K., Pealing, S. L., Miles, C. S., Moysey, R., Taylor, P., Walkinshaw, M. D., Reid, G. A., and Chapman, S. K. (2000) *Biochemistry 39,* 10695−10701] has strengthened the assignment of an arginine (Arg402) as the proton donor in fumarate reduction. Here we describe the crystallographic and kinetic analyses of the R402A, R402K, and R402Y mutant forms of the *Shewanella* enzyme. The crystal structure of the R402A mutant (2.0 Å resolution) shows it to be virtually identical to the wild-type enzyme, apart from the fact that a water molecule occupies the position previously taken by part of the guanidine group of R402. Although structurally similar to the wild-type enzyme, the R402A mutant is inactive under all the conditions that were studied. This implies that a water molecule, in this position in the active site, cannot function as the proton donor for fumarate reduction. In contrast to the R402A mutation, both the R402K and R402Y mutant enzymes are active. Although this activity was at a very low level (at pH 7.2 some 10^4-fold lower than that for the wild type), it does imply that both lysine and tyrosine can fulfill the role of an active site proton donor, albeit very poorly. The crystal structures of the R402K and R402Y mutant enzymes (2.0 Å resolution) show that distances from the lysine and tyrosine side chains to the nearest carbon atom of fumarate are ∼3.5 Å, clearly permitting proton transfer. The combined results from mutagenesis, crystallographic, and kinetic studies provide formidable evidence that R402 acts as both a Lewis acid (stabilizing the build-up of negative charge upon hydride transfer from FAD to fumarate) and a Brønsted acid (donating the proton to the substrate to complete the formation of succinate).

Fumarate reductases are involved in bacterial anaerobic respiration with fumarate acting as a terminal electron acceptor. The majority of these enzymes, which are closely related to succinate dehydrogenase, have been identified as complexes of four (in some cases three) subunits that are anchored to the inner face of the cytoplasmic membrane (*1*, *2*). There are now crystal structures for membrane-bound fumarate reductases from *Escherichia coli* [PDB entry 1FUM (*1*)] and *Wolinella succinogenes* [PDB entries 1QLA and 1QLB (*3*), and 1E7P (*4*)]. The active site for fumarate reduction is located in the flavoprotein subunits of these enzymes, and the crystal structures of several homologous, single-subunit, enzymes have been determined. These include structures with substrate (or substrate-like) molecules bound at the active site in the case of the fumarate reductase from *Shewanella* species [1QJD (*5*) and 1D4E (*6*)]. This soluble enzyme, which has been designated as flavocytochrome c_3 (Fcc_3),[1] is found in the periplasm in contrast to the membrane-bound enzymes which face into the cytoplasm (*7*). Despite these differences in architecture and location, the function of Fcc_3 has been shown to be analogous to that of the membrane-bound enzymes (*8*, *9*). In fact, all of the amino acid residues that have been implicated in substrate binding and catalysis, on the basis of chemical modification and mutagenesis experiments, are conserved between the soluble and membrane-bound enzymes (*10*).

One particular arginine residue in Fcc_3, Arg402 (equivalent to Arg287 and Arg301 in the *E. coli* and *W. succinogenes* enzymes, respectively), has been proposed to be the active site acid/base catalyst for fumarate reduction/succinate oxidation (*11*, *12*). In Fcc_3, the substitution of Arg402 with alanine

† This work was supported by the UK Biotechnology and Biological Sciences Research Council (BBSRC) and by the Wellcome Trust-funded Edinburgh Protein Interaction Centre (EPIC). R.M. acknowledges studentship funding from the BBSRC. D.L. is a postdoctoral fellow of the Fund of Scientific Research-Flanders (Belgium).

* To whom correspondence should be addressed: Department of Chemistry, University of Edinburgh, West Mains Road, Edinburgh EH9 3JJ, U.K. E-mail: S.K.Chapman@ed.ac.uk. Fax and phone: (44) 131 650 4760.

‡ Department of Chemistry.

§ Institute of Cell and Molecular Biology.

[1] Abbreviations: Fcc_3, flavocytochrome c_3; R402A, arginine 402 → alanine mutation; R402K, arginine 402 → lysine mutation; R402Y, arginine 402 → tyrosine mutation; FAD, flavin adenine dinucleotide.

10.1021/bi011360h CCC: $20.00
Published on Web 09/21/2001

resulted in a mutant enzyme which was completely inactive (at the resolution of the assay) over a range of conditions (*11*). Such data are consistent with (but not proof of) this residue being the active site acid catalyst for fumarate reduction.

To further investigate the nature of the active site acid catalyst, we have examined the role of Arg402. In this paper, we describe the kinetic characterization of the R402K and R402Y mutant enzymes. In addition, we report the high-resolution X-ray crystal structures of the R402A, R402K, and R402Y mutant forms of Fcc_3. The combined kinetic and structural data provide unambiguous evidence for the acid catalyst role of R402 in the fumarate reductase mechanism.

MATERIALS AND METHODS

DNA Manipulation, Strains, Media, and Growth. The mutant enzymes R402K-Fcc_3 and R402Y-Fcc_3 were generated by site-directed mutagenesis using the method described by Kunkel and Roberts (*13*). The *fccA* coding sequence was cloned into the phagemid vector pTZ18R (*14*) on an ~1.8 kbp *Eco*RI−*Hin*dIII fragment (*8*) to provide the template.

Mutagenic oligonucleotides CGAAATTACTACTAAA-GATAAAGCATC (in which lysine is substituted for arginine 402) and CGAAATTACTACTTATGATAAAGCATC (in which tyrosine is substituted for arginine 402) were used. Mismatched bases are underlined. Single-stranded DNA was screened for the required mutations using a Perkin-Elmer ABI Prism 377 DNA sequencer. The mutated *fccA* coding regions were fully sequenced from single-stranded DNA to verify that no secondary mutations had been introduced.

To enable expression of R402K and R402Y forms of Fcc_3, the modified coding sequences were cloned individually into the IPTG-inducible, broad-host range expression vector pMMB503EH (*15*) on an ~1.8 kbp *Eco*RI−*Hin*dIII fragment to give pCM88 and pCM107, respectively. Expression in the Δ*fccA Shewanella frigidimarina* strain EG301 (*8*) was as previously described (*11*).

Protein Purification and Kinetic Analysis. Wild-type and mutant forms of Fcc_3 were purified as previously reported (*16*). Protein samples for crystallization were subjected to an additional purification step using FPLC with a Mono Q column as described by Pealing et al. (*17*). Protein concentrations were determined using the Soret band absorption coefficient for the reduced enzyme (752.8 mM^{-1} cm^{-1} at 419 nm) (*16*).

The FAD content of Fcc_3 mutants was determined using the method of Macheroux (*18*), and all steady-state rate constants were corrected for the percentage of FAD present.

Mass spectrometry of proteins was carried out using a Micromass Platform II electrospray mass spectrometer. Samples were prepared in 0.1% formic acid and introduced to the spectrometer via direct infusion. The spectrometer was standardized using horse heart myoglobin.

The steady-state kinetics of fumarate reduction were followed at 25.0 ± 0.1 °C as described by Turner et al. (*19*). The fumarate-dependent reoxidation of reduced methyl viologen was monitored at 600 nm using a Shimadzu UV-PC 1201 spectrophotometer. To ensure anaerobicity, the spectrophotometer was housed in a Belle Technology glovebox under a nitrogen atmosphere with the O_2 level maintained well below 5 ppm. Assay buffers contained 0.45 M NaCl and 0.2 mM methyl viologen and were adjusted to the appropriate pH values using 0.05 M HCl or NaOH as follows: Tris-HCl (pH 7.0−9.0), MES/NaOH (pH 5.4−6.8), and CHES/NaOH (pH 8.6−10). The viologen was reduced by addition of sodium dithionite until a reading of ~1 absorbance unit ($\lambda = 600$ nm) was obtained (corresponding to ~80 μM reduced methyl viologen). The concentration of reduced methyl viologen could be varied between 100 and 20 μM with no effect on the rate of reaction. Fumarate was added to give a range of concentrations (0−350 μM), and the reaction was initiated by addition of a known concentration of the enzyme.

Kinetic parameters K_m and k_{cat} were determined from the steady-state results using non-linear regression analysis (Microcal Origin software).

Crystallization and Refinement. Crystallization of R402A, -K, and -Y mutant flavocytochromes c_3 was carried out by hanging drop vapor diffusion at 4 °C in Linbro plates. Crystals of all mutant flavocytochromes c_3 were obtained with well solutions comprising 100 mM Tris-HCl buffer (pH 7.2−7.8) (measured at 25 °C), 80 mM NaCl, 16−19% PEG 8000, and 10 mM fumarate. Hanging drops (4 μL volume) were prepared by adding 2 μL of 6 mg/mL protein [in 10 mM Tris-HCl (pH 8.5)] to 2 μL of well solution. After ~2 weeks, needles of up to 1 mm × 0.2 mm × 0.2 mm and plates of up to 0.5 mm × 0.5 mm × 0.2 mm were formed.

Crystals were immersed in a solution of 100 mM sodium acetate buffer (pH 6.5), 20% PEG 8000, 10 mM fumarate, and 80 mM NaCl, containing 23% glycerol as a cryoprotectant, prior to mounting in nylon loops and flash-cooling in liquid nitrogen. For R402A and R402K flavocytochromes c_3, data sets were collected to 2.0 Å resolution (Station 9.6, $\lambda = 0.979$ Å for R402A; station 14.2, $\lambda = 1.244$ Å for R402K) at Daresbury synchrotron source using an ADSC Quantum 4 detector. For R402Y flavocytochrome c_3, a data set was collected to 2.0 Å resolution ($\lambda = 1.0332$ Å) on station BM14 at the ESRF in Grenoble using a Mar ccd detector. Crystals of all three mutant forms belong to space group $P2_1$. Crystals of R402A flavocytochrome c_3 were found to have the following cell dimensions: $a = 75.966$ Å, $b = 85.930$ Å, $c = 88.320$ Å, and $\beta = 104.74°$. Those of R402K had the following dimensions: $a = 76.612$ Å, $b = 86.916$ Å, $c = 88.985$ Å, and $\beta = 104.48°$. Those of R402Y had the following dimensions: $a = 78.072$ Å, $b = 87.906$ Å, $c = 90.163$ Å, and $\beta = 105.03°$.

Data processing was carried out using the HKL package (*20*). The wild-type Fcc_3 structure (1QJD), stripped of water, was used as the initial model for molecular replacement. Electron density fitting was carried out using the program TURBO-FRODO (*21*). Restraints for the FAD were calculated from two small molecule crystal structures (Cambridge Crystallographic Database entries HAMADPH and VEFHUJ10). Structure refinement was carried out using Refmac (*22*).

The atomic coordinates have been deposited in the Protein Data Bank [entries 1JRX (R402A), 1JRY (R402K), and 1JRZ (R402Y)].

RESULTS

Characterization of Mutant Enzymes. The molecular masses of the mutant enzymes were determined by electrospray mass spectroscopy (error of ±10 Da) to be lower than that of the wild type (63 033 Da) by 84 Da for R402A (expected difference of 85 Da), 36 Da for R402K (expected

Table 1: Comparison of k_{cat} and K_m Values for Wild-Type, R402K, and R402Y Forms of Fcc_3 (25 °C, $I = 0.45$ M)[a]

	k_{cat} (s^{-1})			K_m (μM)		
pH	wild type[b]	R402K	R402Y	wild type[b]	R402K	R402Y
6.0	658 ± 34	0.02 ± 0.01	0.02 ± 0.01	43 ± 10	18 ± 4	207 ± 25
7.2	509 ± 15	0.06 ± 0.01	0.05 ± 0.01	25 ± 2	66 ± 14	267 ± 44
7.5	370 ± 10	–[c]	0.14 ± 0.01	28 ± 3	–[c]	213 ± 24
9.0	210 ± 13	–[c]	–[c]	17 ± 2	–[c]	–[c]

[a] At the resolution of the assay, the R402A enzyme was inactive under all conditions that were studied. [b] Values for the wild type taken from ref *11*. [c] Reliable data were difficult to obtain at these pH values.

Table 2: Data Collection and Refinement Statistics

	R402A	R402K	R402Y
resolution (Å)	20.0−2.0	20.0−2.0	20.0−2.0
total no. of reflections	711987	538082	744944
no. of unique reflections	74263	79425	76643
completeness (%)	92.4	99.9	96.4
$(I)/[\sigma(I)]$	15.3	16.3	14.3
R_{merge} (%)[a]	7.5	8.7	7.3
R_{merge} in outer shell (%)	20.1 (2.03−2.0 Å)	28.6 (2.03−2.0 Å)	19.7 (2.07−2.0 Å)
R_{cryst} (%)[b]	17.27	16.24	17.51
R_{free} (%)[b]	25.38	23.61	25.49
rmsd from ideal values			
bond lengths (Å)	0.014	0.013	0.014
bond angles (deg)	3.1	2.7	2.9
Ramachandran analysis			
most favored (%)	87.8	88.6	88.4
additionally allowed (%)	12.1	11.4	11.6

[a] $R_{merge} = \sum_h\sum_i|I(h) - I_I(h)|/\sum_h\sum_i I_I(h)$, where $I_I(h)$ and $I(h)$ are the ith and mean measurement of reflection h, respectively. [b] $R_{cryst} = \sum_h|F_o - F_c|/\sum_h F_o$, where F_o and F_c are the observed and calculated structure factor amplitudes of reflection h, respectively. R_{free} is the test reflection data set, ~5% selected randomly for cross validation during crystallographic refinement.

difference of 28 Da), and 5 Da for R402Y (expected difference of 7 Da). All the mutations were further verified by DNA sequencing. The average FAD content of the mutant enzymes was found to be 78% for R402A, 70% for R402K, and 73% for R402Y. This compares with typical values for the recombinant wild-type enzyme of ~73%. All catalytic rates were corrected for the variation in FAD content (*11*).

The ability of R402-substituted forms of Fcc_3 to catalyze fumarate reduction was assessed over a range of pH values. The resulting k_{cat} and K_m parameters for wild-type and mutant forms of Fcc_3 are compared in Table 1. As reported previously (*11*), the R402A mutant enzyme was found to be completely inactive (at least to the sensitivity of the assay) under all conditions. However, some activity was detectable for both the R402K and R402Y forms of Fcc_3 (Table 1). Although this activity was at a very low level (at pH 7.2, the values of k_{cat} for R402K and R402Y were some 10^4-fold lower than that for the wild type), it does imply that both lysine and tyrosine can fulfill the role of active site proton donor, albeit very poorly.

Crystal Structures of the Mutant Flavocytochromes c_3. Data sets to a resolution of 2.0 Å were used to refine the structures to final *R*-factors of 17.27% (R402A; R_{free} = 25.38%), 16.24% (R402K; R_{free} = 23.61%), and 17.51% (R402Y; R_{free} = 25.49%) (Table 2). For each of the mutant enzymes, the final model consists of two protein molecules, each comprised of residues 1−568, four hemes, the FAD, one substrate molecule (fumarate), and one sodium ion. In addition, the R402A model contains 1675 water molecules, the R402K model contains 1841 waters, and the R402Y model contains 1629 waters. Three residues at the C-terminus of the proteins (residues 569−571) could not be located in the electron density maps. The rmsd fit of all backbone atoms for the wild-type and R402A mutant enzyme is 0.5 Å; for the wild-type and R402K enzymes, it is 0.3 Å, and for the wild-type and R402Y enzymes, it is 0.4 Å, indicating no major differences between the four structures. Due to the fact that the crystallographic models for the mutant enzymes have two molecules in the asymmetric unit, the rmsd fit values stated represent the mean value over both molecules. In addition, the rmsd fit between both molecules (A and B) in the asymmetric unit is ~0.2 Å for all the mutant enzyme structures.

Wild-type, R402A, R402K, and R402Y flavocytochromes c_3 were all crystallized in the presence of 10 mM fumarate. In the crystal structures of the R402 substituted enzymes, fumarate is bound at the active site in a twisted conformation similar to that observed for the C2-hydroxylated substrate-like molecule found at the active site of the wild-type enzyme (*5*). The major difference in the active sites of the mutant enzymes is the replacement of the arginine at position 402 with alanine, lysine, or tyrosine. The active sites of the R402A, R402K, and R402Y enzymes are shown in panels a−c of Figure 1, respectively, while an overlay of the mutant enzyme active sites with that of the wild-type enzyme is shown in Figure 2. In the case of the R402A mutant enzyme, replacement of arginine with alanine results in an inactive enzyme (*11*). It can clearly be seen that in the active site of the R402A enzyme the presence of alanine at position 402 removes the functionality responsible for proton transfer, and the smaller volume of the alanine side chain allows entry of a water molecule into the active site (Figure 1a). This water molecule (WAT398 in molecule A and WAT375 in molecule B) is found to lie between A402 and the bound substrate molecule 4.5 Å from the A402 methyl carbon and 4.0 Å from the C3 atom of fumarate. This water molecule is also found to be within hydrogen bonding distance of the side chain oxygen of Q363 (2.7 Å) and the C4 carboxylate moiety of the bound substrate (2.9 Å). In the R402A structure, it is also clear that the putative proton delivery pathway involving R381, E378, and R402 [proposed by Doherty et al. (*11*)] adopts a slightly different conformation. The distance between the side chains of R381 and E378 is 4.2 Å, compared to 3.1 Å in the wild-type enzyme, while the distance between the side chain of E378 and the active site water is 4.5 Å. In addition, in the structure of the R402A enzyme, there is a slight movement of the protein backbone around position 402 toward the substrate, relative to that of the wild-type enzyme, which accounts for the higher rmsd backbone fit value mentioned above.

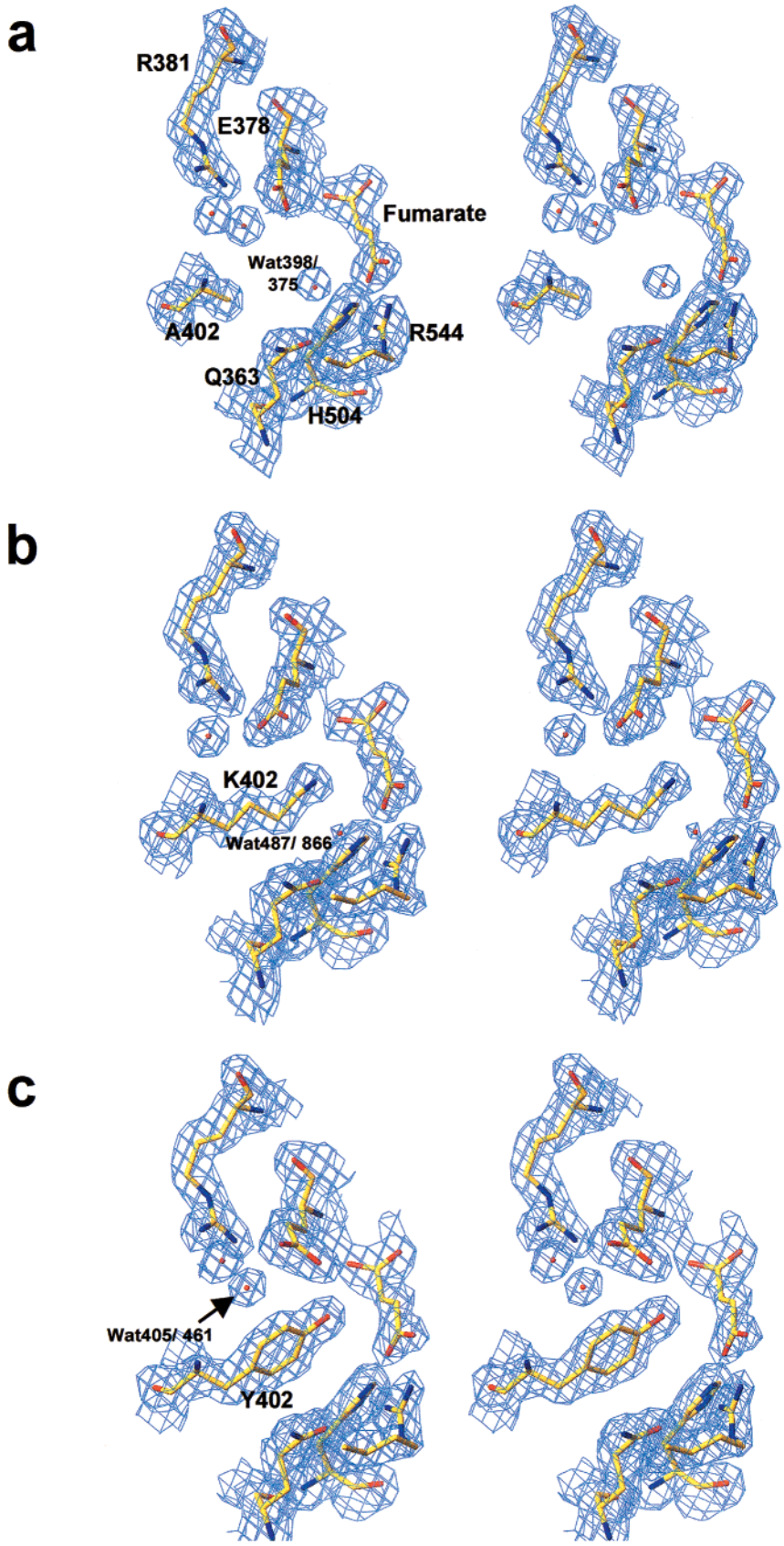

FIGURE 1: Stereodiagrams of the active sites of the (a) R402A, (b) R402K, and (c) R402Y mutant flavocytochromes c_3. The orientations of all three are the same, and the labeling in panel a is applicable to all, with the exception of the identity of the residue at position 402 and the water molecules. Electron density was computed using the Fourier coefficients $2F_o - F_c$, where F_o and F_c are the observed and calculated structure factors, respectively, the latter based on the final model. The contour level is 1σ, where σ is the rms electron density. This diagram was generated using TURBO-FRODO (*21*).

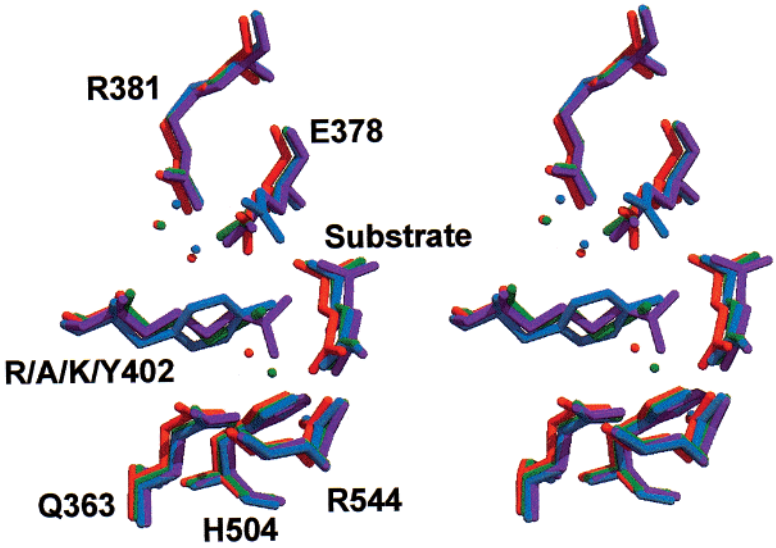

FIGURE 2: Stereodiagram of the overlaid active sites of the wild-type (purple), R402A (red), R402K (green), and R402Y (blue) enzymes, showing the proximity of the proton-donating species to the bound substrate molecules and the positions of the active site waters in each structure. This diagram was generated using MOLSCRIPT (*25*) and Raster 3D (*26*).

In the structure of the R402K mutant enzyme, the K402 side chain is seen to occupy a position similar to that taken by the arginine in the wild-type enzyme (Figures 1b and 2). This results in a proton transfer distance of 3.7 Å between the lysine side chain amino group and the C3 of bound fumarate, compared to a distance of 3.0 Å (from the R402 side chain amino to substrate C3) in the wild-type enzyme. In the R402K mutant enzyme, the proton delivery pathway is similar to that in the wild-type enzyme with proton transfer distances of 2.9 Å (from R381 to E378) and 3.4 Å (from E378 to K402). It should be noted, however, that as in the R402A enzyme a water molecule is also found near the active site which is not present in the wild-type enzyme. This water (WAT487 in molecule A and WAT866 in molecule B) is, like that found in the R402A active site, H-bonded to the side chain O of Q363 at a distance of 2.9 Å, and is 2.8 Å from the terminal amino group of the K402 side chain.

In the case of the R402Y enzyme, the side chain of Y402 adopts a position so that the hydroxyl group is 3.2 Å from the substrate C3 atom (Figure 1c), thus enabling proton transfer during catalysis. In this case, however, the proton delivery pathway is perturbed by a change in the position of the E378 side chain which remains only 3.0 Å from the side chain hydroxyl of Y402, but is 5.4 Å from the R381 side chain. It appears that this movement has allowed a water molecule (WAT405 in molecule A and WAT461 in molecule B) to position between R381 and E378, 2.8 Å from the R381 side chain amino group and 4.0 Å from the E378 side chain carboxylate, a position which could allow it to mediate in the proton delivery process.

In addition to all the structural features mentioned here, it should be noted that in all cases substitution at position 402 has a minimal effect on the hydride transfer distance between the substrate C2 atom and the FAD N5 atom, with values ranging between 3.4 and 3.6 Å for all enzymes being discussed here.

DISCUSSION

The proposed mechanism for fumarate reduction is shown in Figure 3. Since the active sites in all of the known fumarate

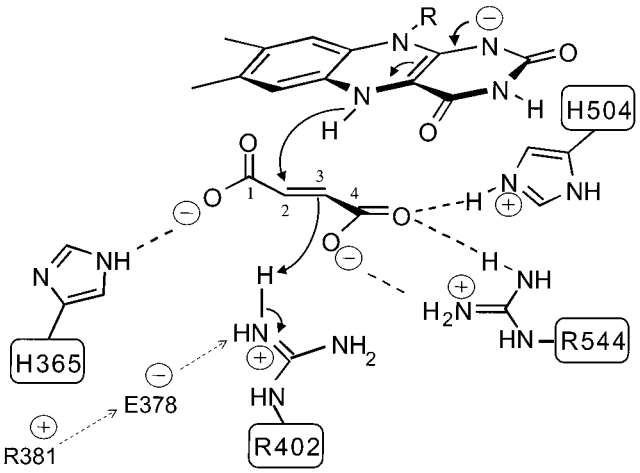

FIGURE 3: Reaction mechanism for fumarate reduction [this is an abbreviated version of the mechanism proposed by Taylor et al. (*5*)]. The substrate is polarized by interactions with charged residues facilitating hydride transfer from N5 of the reduced FAD to C2 of the substrate. Arg402 is ideally positioned to donate a proton to C3 of the substrate, resulting in the formation of succinate. Arg402 is immediately reprotonated via a proton pathway involving Arg381 and Glu378.

reductase structures (*1*, *3*−*6*, *23*) are well-conserved, it is our strong belief that this mechanism operates in all members of the fumarate reductase family. In addition, it is now clear that this mechanism is also applicable to fumarate reduction by the enzyme L-aspartate oxidase from *E. coli* (*24*), an enzyme that is substantially structurally similar to the soluble fumarate reductases.

Although there has been general agreement that hydride transfer from N5 of the FAD cofactor to the substrate is a key step in the mechanism for fumarate reduction, there has been some debate about the identity of the proton donor required to complete the formation of succinate. The original idea that a histidine might have been the proton donor (*10*) has been categorically ruled out by a combination of crystallographic and mutagenesis studies (*11*). Lancaster and co-workers (*3*), based on their initial crystal structure of the *Wolinella* fumarate reductase, made the suggestion that a

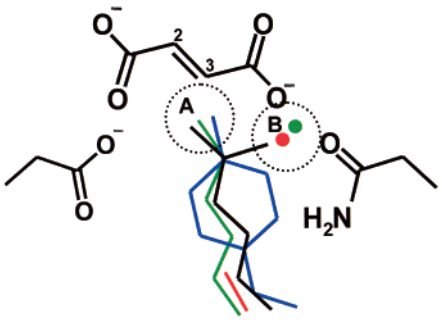

FIGURE 4: Schematic representation of sites A and B in the active site of flavocytochrome c_3. The figure shows fumarate at the top, with atoms C2 and C3 appropriately labeled, E378 at the left, and Q363 at the right. The residues at position 402 in each structure are shown as arginine (black), alanine (red), lysine (green), and tyrosine (blue). It can clearly be seen that the proton-donating species on each side chain fall within the region defined as A, while position B is occupied by the other NH_2 group of R402, and by water molecules in the R402A and R402K enzymes (represented by red and green circles, respectively).

water molecule might function as the catalytic proton donor. This proposal was challenged (*11*), since the active site water molecule seen in the structure of the *Wolinella* enzyme was absent from all the other substrate-bound fumarate reductase structures (*1*, *5*, *6*). An alternative explanation was put forward, that being that the *Wolinella* enzyme had crystallized in a partially open, catalytically inactive, form (*11*, *12*). It was further suggested that had the *Wolinella* enzyme crystallized in the closed, catalytically active, form then the position of the water molecule would have been occupied by an arginine side chain as in all the other fumarate reductase structures (*11*). More recently, Lancaster et al. (*4*) have succeeded in preparing a third crystal form of the *Wolinella* enzyme which was much more similar to those of fumarate reductases from other organisms than to that found in previous crystal forms of the *Wolinella* enzyme. These authors now agree that it is indeed an arginine residue and not a water molecule that functions as the active site acid.

Further evidence that water might be unlikely to perform the function of an active site acid catalyst comes from our results on the R402A Fcc_3. Why does this particular substitution result in a total loss of activity? Clearly, the guanidinium group of R402 provides an additional function that a water molecule cannot. In Figure 4, the two NH_2 groups of the guanidinium moiety of R402 are labeled as occupying sites A and B. The NH_2 at site A clearly interacts with the substrate C3 atom, whereas the NH_2 at site B interacts with an oxygen from the C4 carboxylate group of fumarate. In the mechanism shown in Figure 3, hydride transfer leads to the buildup of negative charge around the C3 and C4 atoms of the substrate which would be greatly facilitated by the double interaction provided by the guanidinium group of the arginine. In other words, the arginine is acting as a powerful Lewis acid. The arginine can then protonate at the substrate C3 atom by using the NH_2 group at site A as a Brønsted acid (Figure 4).

In contrast to what is observed in the crystal structure of the wild-type enzyme, the structure of the R402A mutant enzyme reveals a water molecule at site B (Figure 4), some 4.0 Å from the C3 atom of fumarate and 2.9 Å from the C4 carboxylate. In this location, the water molecule is involved

Enzyme	Mean Distance (Å)[a]						
	1	2	3	4	5	6	7
Wild-Type	3.0	3.4	3.0	3.3	3.1	2.8	3.6
R402A	na	3.4	2.7	na	4.2	na	2.9
R402K	3.7	3.4	2.9	3.4	2.9	3.7	3.4
R402Y	3.2	3.5	na	3.0	5.4	3.4	na

[a] Numbers in bold type represent distances between atoms in each structure as indicated below

1) Proton donor species (position A) and substrate C3.
2) Substrate C2 and FAD N5.
3) Q363 side chain amide O and the species occupying position B in each structure.
4) The side chain O of E378 and the proton donor species.
5) The side chain terminal N of R381 and the side chain O of E378.
6) The atom occupying position A and the substrate C4-carboxylate O.
7) The atom occupying position B and the substrate C4-carboxylate O.

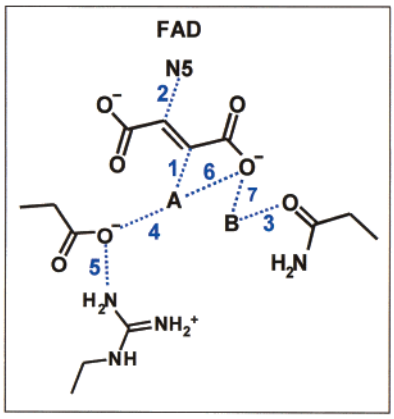

FIGURE 5: Important interatomic distances in Fcc_3 crystal structures. The figure shows a schematic representation of the distances described in the table.

in a hydrogen bonding interaction with Q363 (and also possibly with a substrate carboxylate oxygen) and, in such a position, is simply unable to function as a proton donor. It is possible, however, that if the water molecule had occupied position A in Figure 4, then it may have been able to act as a proton donor. Thus, in the R402A mutant enzyme, although water should be able to function as a Brønsted acid, it occupies a position which precludes it from doing so.

From the schematic representation of sites A and B shown in Figure 4, it can also be seen that the side chain amino group of K402 occupies site A, 3.7 Å from the substrate C3 atom and 3.7 Å from the C4 carboxylate of the bound substrate, while a water molecule occupies position B within hydrogen bonding distance of both Q363 and K402.

In the case of the R402Y mutant enzyme, the Y402 side chain is positioned so that the proton-donating hydroxyl group lies in position A, 3.2 Å from the substrate C3 atom and 3.4 Å from the C4 carboxylate of the bound substrate. There is no molecule occupying position B in the active site of the R402Y enzyme. Interestingly, the proton transfer distance from E378 to Y402 is, at 3.0 Å, shorter than that observed in the other catalytically active enzymes described here, but the proton transfer distance between R381 and E378 is greatly increased to 5.4 Å. However, there is a water molecule (WAT405/461) between these two side chains which could facilitate proton delivery to the active site Brønsted acid.

In summary, the structural data enable the identification of two distinct sites, A and B, as occupied by the two terminal N atoms of the side chain of R402. Only if a species capable of functioning as a Brønsted acid occupies position

A will proton transfer to the substrate occur, and the fact that both R402Y and R402K enzymes have similar k_{cat} values suggests that a positive charge in this position is unnecessary. The species occupying position B cannot act as a proton donor but can, in the case of the arginine side chain, act to stabilize the build-up of negative charge in the transition state by functioning as a Lewis acid. It can be seen clearly from Figure 2 that the proton-donating side chains of R402, K402, and Y402 do indeed reside in position A, resulting in measurable enzymatic activity. Although positions A and B are occupied in the R402K enzyme, the water molecule in position B is unable to function as a Lewis acid, and it may be postulated that this lack of transition-state stabilization is at least partially responsible for the low catalytic rate of this enzyme. In contrast, in the structure of the R402A mutant enzyme, there is nothing appropriately positioned to transfer a proton to the substrate, and only position B is occupied, in this instance by a water molecule. All the important distances between the substrate and the species occupying positions A and B in the four structures discussed here are tabulated in Figure 5, which also contains the measured distances in the proton delivery pathway for each enzyme.

It is also interesting to note that in L-aspartate oxidase, the substitution of the equivalent arginine (R290 in this case) with a leucine also leads to a complete loss of activity, even though fumarate binds tightly to the mutant enzyme (*24*). This supports our conclusion that site A must be occupied by a species capable of Brønsted acid function for measurable catalysis to occur. The combined kinetic and structural information obtained from the mutant enzymes described in this paper provides a clear description of the details of the mechanism of fumarate reduction. The efficiency of Arg402 as the active site catalyst in the wild-type enzyme is justified in terms of its unique ability to simultaneously occupy positions A and B and to act as both a Brønsted acid and Lewis acid in each site, respectively.

ACKNOWLEDGMENT

We thank SRS Daresbury and the BM14 beamline at the ESRF in Grenoble for use of synchrotron facilities.

REFERENCES

1. Iverson, T. M., Luna-Chavez, C., Cecchini, G., and Rees, D. C. (1999) *Science 284*, 1961−1966.
2. Körtner, C., Lauterbach, F., Tripier, D., Unden, G., and Kröger, A. (1990) *Mol. Microbiol. 4*, 855−860.
3. Lancaster, C. R. D., Kröger, A., Auer, M., and Michel, H. (1999) *Nature 402*, 377−385.
4. Lancaster, C. R. D., Gross, R., and Simon, J. (2001) *Eur. J. Biochem. 268*, 1820−1827.
5. Taylor, P., Pealing, S. L., Reid, G. A., Chapman, S. K., and Walkinshaw, M. D. (1999) *Nat. Struct. Biol. 6*, 1108−1112.
6. Leys, D., Tsapin, A. S., Nealson, K. H., Meyer, T. E., Cusanovich, M. A., and Van Beeumen, J. J. (1999) *Nat. Struct. Biol. 6*, 1113−1117.
7. Morris, C. J., Black, A. C., Pealing, S. L., Manson, F. D. C., Chapman, S. K., Reid, G. A., and Ward, F. B. (1994) *Biochem. J. 302*, 587−593.
8. Gordon, E. H. J., Pealing, S. L., Chapman, S. K., Ward, F. B., and Reid, G. A. (1998) *Microbiology 4*, 937−945.
9. Reid, G. A., Gordon, E. H. J., Hill, A. E., Doherty, M., Turner, K., Holt, R., and Chapman, S. K. (1998) *Biochem. Soc. Trans. 26*, 418−421.
10. Schröder, I., Gunsalus, R. P., Ackrell, B. A. C., Cochran, B., and Cecchini, G. (1991) *J. Biol. Chem. 266*, 13572−13579.
11. Doherty, M. K., Pealing, S. L., Miles, C. S., Moysey, R., Taylor, P., Walkinshaw, M. D., Reid, G. A., and Chapman, S. K. (2000) *Biochemistry 39*, 10695−10701.
12. Reid, G. A., Miles, C. S., Moysey, R. K., Pankhurst, K. L., and Chapman, S. K. (2000) *Biochim. Biophys. Acta 1459*, 310−315.
13. Kunkel, T. A., and Roberts, J. D. (1987) *Methods Enzymol. 154*, 367−382.
14. Rokeach, L. A., Haselby, J. A., and Hoch, S. O. (1988) *Proc. Natl. Acad. Sci. U.S.A. 85*, 4832−4836.
15. Michel, L. O., Sandkvist, M., and Bagdasarian, M. (1995) *Gene 152*, 41−45.
16. Pealing, S. L., Cheesman, M. R., Reid, G. A., Thomson, A. J., Ward, F. B., and Chapman, S. K. (1995) *Biochemistry 34*, 6153−6158.
17. Pealing, S. L., Lysek, D. A., Taylor, P., Alexeev, D., Reid, G. A., Chapman, S. K., and Walkinshaw, M. D. (1999) *J. Struct. Biol. 127*, 76−78.
18. Macheroux, P. (1999) in *Flavoprotein Protocols: Methods in Molecular Biology* (Chapman, S. K., and Reid, G. A., Eds.) Vol. 131, pp 1−7, Humana Press, Totowa, NJ.
19. Turner, K. L., Doherty, M. K., Heering, H. A., Armstrong, F. A., Reid, G. A., and Chapman, S. K. (1999) *Biochemistry 38*, 3302−3309.
20. Otwinowski, Z., and Minor, W. (1997) *Methods Enzymol. 276*, 307−326.
21. Roussel, A., and Cambillau, C. (1991) TURBO-FRODO, in *Silicon Graphics Geometry Partners Directory 86*, Silicon Graphics, Mountain View, CA.
22. Murshudov, G. N., Vagin, A. A., and Dodson, E. J. (1997) *Acta Crystallogr. D53*, 240−255.
23. Bamford, V., Dobbin, P. S., Richardson, D. J., and Hemmings, M. (1999) *Nat. Struct. Biol. 6*, 1104−1107.
24. Tedeschi, G., Ronchi, S., Simonic, T., Treu, C., Mattevi, A., and Negri, A. (2001) *Biochemistry 40*, 4738−4744.
25. Kraulis, J. (1991) *J. Appl. Crystallogr. 24*, 946−950.
26. Merrit, E. A., and Murphy, M. E. P. (1994) *Acta Crystallogr. D50*, 869−873.

BI011360H